Title: Selective and sensitive onsite detection of phthalates in common solvents

Authors: Shishir Venkatesh[1, +], Chi-Chung Yeung[2, +], Qi-Jun Sun[1], Jiaqing Zhuang[1], Tan Li[1], Robert K.Y. Li[1], Roy Vellaisamy[1,*].

All correspondences should be sent to Dr. Roy Vellaisamy (email: val.roy@cityu.edu.hk)

Affiliations

[1]Department of Physics & Material Science, City University of Hong Kong, 83 Tat Chee Avenue, Kowloon, Hong Kong, S.A.R.

[2] Department of Biology & Chemistry, City University of Hong Kong, 83 Tat Chee Avenue, Kowloon, Hong Kong, S.A.R.

Abstract

Phthalates, which are proven to have adverse health effects, are globally restricted for use in all kinds of plastics through various regulations. Although there are laboratory based techniques for phthalate detection, there is a pressing need for a field based technique so samples can be pre-screened. Here, we report a molecularly imprinted polymer (MIP) functionalized extended gate field effect transistor (EGFET) as a field sensor to identify di-2-ethlyhexyl phthalate (DEHP), which is the one of the most commonly used phthalate. In DI water, DEHP is detected at the extremely low concentration of 25 μg/L while exhibiting excellent selectivity. We are able to tune the linear dynamic range of the sensor by synthesizing the MIP with a different monomer-

to-template ratio and by choice of the functional monomer. Finally, the sensor is calibrated for DEHP in artificial saliva at sub 50 μg/L, showing applicability in phthalate migration tests, which are used in assessing the safety of plastic toys. Furthermore, our sensor platform can be further extended to identify other phthalates as fast pre-screening tool.

1.0 Introduction

Phthalates are a family of chemicals that are used as plasticizers in polymers such as poly-vinyl chloride (PVC). They are found in a wide range of products from construction materials and electrical wire shielding to toys and food packaging. Broadly speaking, the phthalates are classified into low molecular weight and high molecular weight based on the number of carbon in the backbone chain. Low molecular weight phthalates such as dibutyl phthalate (DBP) are commonly used as solvents and plasticizers in personal care items such as nail polish. They have largely been banned by regulatory bodies [1] due to their role in endocrine disruption [2]. Among the high molecular weight phthalates, the most commonly used are di-2-ethylhexyl phthalate (DEHP) and di-isononyl phthalate (DINP). Although their use is widespread in PVC containing products, there have been concerns with regards to the detrimental effects on human health caused by exposure to these chemicals. DEHP in particular has been linked to human reproductive organ toxicity that inhibits their development [3, 4]. Therefore, the use of DEHP is completely banned in children's toys in the European Union [5] and in the United States (CPSIA, 2008). In addition, there have been limits set on the migration of DEHP in food contact materials (EC/10/2011). Despite the rules, there have been instances where large sections of the population have been exposed to DEHP exceeding the limits such as in the 2011 Taiwan food scandal [6]. As such, it becomes of paramount importance to measure and monitor the concentration level of DEHP in various products so as to ensure consumer safety.

Presently, the techniques for the detection of DEHP are purely laboratory based with the most common procedure being gas chromatography (GC). GC is used to separate a mixture of organic compounds followed by quantification by an instrument such as a mass spectrometer (MS). GC-MS has been successfully used to quantify DEHP in liquid samples in several studies [7-12]. Leng et al. reported on GC-MS technique that was preceded by a vortex-assisted liquid-liquid micro-extraction that achieved a detection limit of 9 ppt for DEHP [13]. GC has also been coupled with other instruments such as electron capture detector (ECD) [14] for DEHP detection in water and flame ionization detector (FID) [15] for DEHP detection in beer. High performance liquid chromatography (HPLC) is another laboratory-based technique used in the detection of DEHP in liquid samples. It is coupled with UV [16] for environmental water samples and mass-spectrometer (MS) for urine [17, 18] and wine samples [19].

While these analytical techniques are accurate and sensitive, they require expensive instrumentation, stringent sampling procedures and trained personnel for operation. There is a growing demand for non-laboratory based techniques that can be employed as a pre-screener. Zia et al. have successfully demonstrated DEHP detection in water samples using electro-impedance spectroscopy (EIS) in several studies [20-23]. The sensing principle lies in the detection of changing impedance of the material-under-test (MUT) when exposed to different concentrations of DEHP. In their latest study [23], a molecularly-imprinted polymer (MIP) was used as the MUT. MIPs are polymers that have been synthesized in the presence of target molecules or templates. Removal of the template subsequent to polymerization leaves cavities where specific binding can take place. The MIP is then employed as the receptor in sensors, making the sensors selective towards a specific analyte. While these impedimetric sensors developed by Zia et al. can be easily installed in an industrial environment, they still require the use of high frequency

(100 kHz) circuitry and impedance analyzers which makes them incompatible with portable technology.

An alternative method that can sense the changing impedance of a dielectric medium is the field effect transistor (FET). In this technique, the MUT forms the insulating layer between the gate electrode and the semiconducting channel. A change in the capacitance of the dielectric MUT modulates the source-drain current of the FET. FETs can be operated in DC and also offer in-built signal amplification [24]. This makes them ideal candidates for portable technologies. Contemporary FETs are fabricated using silicon semiconductor technology but they can also be fabricated using organic semiconductors to make organic field effect transistors (OFET). However, organic materials degrade when exposed to aqueous solutions. An extended gate structure, in which the organic semiconductor is isolated from the sample, circumvents this issue. In this study, an extended gate organic field effect transistor (EG-OFET) with the extended gate coated with DEHP imprinted polymer is used to detect DEHP mixed in liquid samples.

2.0 Materials and methods

2.1 Materials: Heavily doped silicon substrates were purchased from University Wafers, USA. Hafnium (IV) chloride, hexamethyldisilazane (HMDS), Copper hexadecafluorophthalocyanine (F_{16}CuPc) and di-2-ethylhexyl phthalate (DEHP) were purchased from Sigma-Aldrich, USA. Gold pellets for thermal evaporation were purchased from Kurt Lesker, USA. Functional monomers acrylamide and acrylic acid were purchased from Sigma-Aldrich, USA. N,N-methylene-biacrylamide, dimethlyformamide, tetramethylethylenediamine (TEMED) and ammonium persulfate were purchased from Sigma-Aldrich, USA. Di-2-ethlyhexyl phthalate, dioctyl sebacate and di-n-hexyl phthalate were purchased from Sigma-Aldrich, USA. Polydimethylsiloxane (PDMS) (Sylgard184®) was purchased from Dow Corning, USA. Sodium

dioctyl sulfosuccinate, sodium chloride, potassium chloride, sodium sulphate, ammonium chloride, urea and lactic acid was purchased from Sigma-Aldrich, USA. Acetone, ethanol and n-hexanol used were of reagent grade purchased from Sigma-Aldrich, USA. Deionized (DI) water (resistivity: 18.2 MΩ .cm) was obtained from a MilliQ system (Millipore, USA).

2.2.1 OFET Fabrication: The bottom gate-top contact OFET was fabricated using a previously reported procedure [25]. Heavily doped silicon wafers were cut into 1.5 cm x 1.5 cm squares. They were then successively cleaned in deionized water, acetone and ethanol baths by ultrasonic cleaner. 0.1 M hafnium (IV) chloride solution was prepared by dissolving hafnium chloride powder in ethanol and stirring the mixture for 2 hours. The solution was subsequently spin-coated (3000 rpm, 40 seconds) on the cleaned silicon substrates and the solvent was evaporated on a hot plate at 120°C. Upon removal of the solvent, the substrates were placed in a 500°C furnace for 2 hours to oxidize the hafnium chloride to hafnium oxide. The thickness of the hafnium oxide layer was approximately 10nm measured via ellipsometry. HMDS, which improves the electrical performance of the OFET, was spin coated to modify the surface of the oxide layer. Thereafter, 30 nm of $F_{16}CuPc$ n-type organic semiconductor was deposited via thermal evaporation in a vacuum (4 x 10^{-6} mbar) chamber. Finally, 50 nm thick gold source and drain electrodes were patterned via thermal evaporation through a shadow mask. The OFET fabrication procedure is illustrated in Fig. 1a

2.2.2 DEHP imprinted polymer synthesis: The DEHP imprinted polymer was synthesized using a previously reported procedure [23]. The molecular-imprinted polymer was first prepared by mixing 14.5mmol functional monomer acrylamide, 5.3mmol cross-linker N,N-methylene-biacrylamide, 0.7 mmol ammonium persulfate and 2.5mmol template (analyte) di-2-ethylhexyl phthalate (DEHP) in 25mL Dimethylformamide and 10 mL DI water. After the solution was well

mixed, the solution was degassed by nitrogen. 0.5mL tetramethylethylenediamine (TEMED) was added to initiate the polymerization. The solution was kept for 16hr in order to complete the polymerization to form poly-acrylamide. MIP was filtered, washed and dried under nitrogen atmosphere. Then, MIP was ground and sieved to obtain 50µm sized particles. The DEHP template was extracted out from the MIP by the Soxhlet extraction in 24hr with methanol. Finally, the MIP powder was dried under a nitrogen atmosphere.

2.2.3 Extended gate sensor fabrication: Heavily doped silicon wafers were cut into 1.5 cm x 1.5 cm squares. They were then successively cleaned in deionized water, acetone and ethanol baths by ultrasonic cleaner. 1 mg of MIP powder was mixed with 1 mL of tricholoromethylsilane and drop casted onto the cleaned silicon wafer surface. The solution usually dried in about 5 minutes. Finally, a polydimethylsiloxane (PDMS) well was patterned on the surface of the MIP to hold the sample over a defined area of about 1 cm_2. The fabrication of the extended gate sensor is illustrated in Fig. 1b.

2.3.1 Sample Preparation: Standard solutions of varying DEHP concentration were prepared by performing serial dilutions of DEHP in deionized water, ethanol, n-hexanol and artificial saliva. Artificial saliva was prepared in accordance with BS 6684. 0.45 g sodium chloride, 0.03 g potassium chloride, 0.03 g sodium sulphate, 0.04 g ammonium chloride, 0.02 g urea and 0.3 g lactic acid were mixed in 100 mL deionized water to make artificial saliva.

2.3.2 Testing Methodology: The bottom gate of the OFET was electrically connected to the bottom of the extended gate sensor as shown in Fig. 2. 10 µL of the sample was pipetted onto the surface of the MIP coated extended gate sensor. A source-measurement unit (SMU, Keithley 2612A) was used to apply a 3V gate voltage (V_{GS}) to a gold plated reference electrode immersed in the sample. The same SMU was used to apply a 3V drain voltage (V_{DS}) to the OFET via

connected probes. The source-drain current (I_{DS}) was measured as a function of sample concentration. The measurement was continued until a stable reading was achieved. Calibration was performed by measuring the source-drain current upon exposure to increasing concentrations of the analyte. A LabTracer program interfaced with the SMU was used for data acquisition. Contact angle measurements were made using a contact angle goniometer (rame-hart, Model 200).

3.0 Results and Discussion

The response of the sensor is characterized by the change in the source-drain current in the OFET, which is expressed in the form of normalized current (N.C.) which is defined as $N.C. = \frac{I_{DS} - I_{DS,0}}{I_{DS,0}}$ where I_{DS} is the source-drain current at the given concentration and $I_{DS,0}$ is the source-drain current at zero analyte concentration.

3.1 Effect of dilution solvent: The response of the sensor to DEHP dissolved in three different solvents, namely ethanol, n-hexanol and water have successively been characterized in that order. Ethanol was initially chosen as the solvent because of the excellent miscibility of DEHP in ethanol. However, as seen in the Fig. 3, there is almost no change observed in the N.C. upon exposure to different DEHP concentrations. The reason for this is hypothesized to be caused by the affinity of DEHP to ethanol. This results in insufficient energy for the DEHP molecules to de-solvate from ethanol and fill the empty voids within the MIP i.e. there is a poor analyte capture. Subsequently, n-hexanol is chosen as the solvent as it contains the same functional group as ethanol but with a longer carbon backbone. It is speculated that the higher viscosity of the solvent would reduce the energy required for de-solvation thereby improving the efficiency of analyte capture. As predicted, the sensor shows a response to DEHP concentrations beyond 100 µg/L. In fact, a near-linear relation between the N.C. and DEHP concentration is observed

between 100 µg/L and 100000 µg/L. The results for the n-hexanol test are presented in Fig. 3. However, as DEHP is a banned chemical, a more sensitive response is desired. Therefore, de-ionized (DI) water is chosen as the solvent due to its non-affinity towards DEHP. As seen in Fig. 3, the sensors exhibit a distinguishable response even at a trace concentration of 25 µg/L. This implies a very efficient analyte capture. However, there is a downside to this efficient capture. The voids within the MIP become saturated when the analyte concentration reaches 50 µg/L. This is evidenced by the no change in sensor response after exposing to higher concentrations of DEHP. The extreme sensitivity of the sensor to DEHP dissolved in DI water is also evident in the magnitude of the N.C. in Fig. 3. The maximum value of N.C. is 0.8 in DI water while it is only around 0.35 in n-hexanol. Thus, it is inferred that DI water is the optimal solvent to dilute DEHP samples for further sensor characterization experiments presented in this article.

3.2 Calibration curve of sensor with DEHP samples dissolved in DI water: The sensor is calibrated against more points with the DEHP (mixed with DI water) samples. The results from this test are presented in Fig. 4. As seen in the figure, the sensor shows almost no response for concentrations below 15 µg/L. Beyond this point, a sharp increase in the N.C. can be observed. However, after reaching 50 µg/L, no further increase in the current is observed. This is possibly due to the saturation of the voids within the MIP. After this point, the sensor becomes unresponsive to further increase in analyte concentration. The advantage of this sensor is its extreme sensitivity i.e. its ability to detect DEHP concentrations at sub 50 µg/L levels. However, it can be seen from the calibration curve that the sensor suffers from a narrow linear dynamic range which is between 25 µg/L and 50 µg/L.

3.3 Selectivity: To confirm whether the signal originated from physio-adsorption or from the specific binding of analyte in the MIP void, the selectivity is tested. In this test, the calibration

curves are acquired for two other plasticizers, namely di-n-hexyl phthalate (DnHP) and dioctyl sebacate (DOS) diluted in DI water. The results from this test are presented in figure 5. The sensor is almost non-responsive to di-n-hexyl phthalate (DnHP) and dioctyl sebacate (DOS), while it shows a distinguishable response when exposed to the target analyte DEHP. From this, it is concluded that the origination of the signal is from the specific binding of the DEHP molecule within the MIP voids.

3.4 Proposed model for sensing mechanism: Based on the previous tests, a model for sensing mechanism is proposed. But first, it is important to characterize the working of the OFET. The current in the OFET channel is modulated by the voltage applied at the gate. In all the tests performed in the previous sections, the OFET operates in saturation mode. The equation for the source-drain current in saturation mode is $I_{DS,Max} = \frac{W}{2L}\mu C_i(V_{GS}-V_T)^2$, where $I_{DS,Max}$ is the saturation mode source-drain current, μ is the mobility, C_i is the gate capacitance, V_{GS} is the gate-source voltage and V_T is the threshold voltage. As seen in the I_{DS}-V_{GS} figure (Fig. 6), the threshold voltage decreases as the concentration of the analyte increases. Consequently, the saturation source-drain current increases as the concentration increases. However, the physical meaning behind this threshold voltage shift needs to be elucidated.

To explain the threshold voltage shift, we must first consider the electrical layout of the sensor. The MIP and the dielectric oxide layer (HfO_2 layer), are electrically connected in series. The equation for the threshold voltage shift (ΔV_T) in this system is modified to $\Delta V_T = \left(\frac{C_{MIP}+C_{OX}}{C_{MIP}C_{OX}}\right) Q_{SEMI}$ where C_{MIP} & C_{OX} are the capacitances of the MIP and the OFET dielectric oxide respectively and Q_{SEMI} is the induced charges in the OFET semiconductor [26]. The only parameter that is influenced by exposure to the analyte is C_{MIP}. C_{MIP} is defined as $C_{MIP} = \frac{\varepsilon_o \varepsilon WL}{t}$ where ε_o is the vacuum permittivity, ε is the relative permittivity (dielectric constant), W, L & t

are the width, length and thickness of the MIP respectively. Upon exposure to the sample, the specific analyte occupies the voids within the MIP layer resulting in morphological changes [27]. The binding of the analyte in the MIP layer is illustrated in Fig. 7. Accordingly, there is an increase in the relative permittivity and the capacitance of the MIP layer. This leads to the threshold voltages shifting to lower values with increasing analyte concentrations. This sensing principle has been employed in other MIP based sensors where the change in capacitance or dielectric constant is measured directly [28-31].

3.5.1 Effect of increasing the MIP loading: In order to improve the linear dynamic range of the sensor, the MIP loading was increased. The MIP loading is defined as: MIP loading= $\frac{\text{Mass of MIP (mg)}}{\text{Volume of Trichloromethylsilane (mL)}}$. The MIP loading was changed from 1mg/mL to 5 mg/mL. It was postulated that increasing the MIP loading would provide more sites for the analyte to bind thereby allowing for a larger dynamic range. However, as shown in Fig. 8, there is absolutely no change in the linear dynamic response range of the sensor. It is also observed that the surface of the MIP became relatively more hydrophobic with the increased MIP loading (see Fig. 9b & 9c). It is rationalized that the increased hydrophobicity reduced the contact area between the sample and the MIP, causing reduced occupation of binding sites. In order to increase the contact area, the DEHP samples were mixed with a 0.5% surfactant (sodium dioctyl sulfosuccinate) (see Fig. 9e & 9f). However, as seen in Fig. 8, the increase in contact area only produces an increase in the magnitude of the signal (i.e. magnitude of I_{DS}) but no change in the linear dynamic range. Also, the increase in I_{DS} at zero analyte concentration leads to the reduced N.C. From these results, it is inferred that increasing the MIP loading has no effect on the linear dynamic range even after the mixing of the sample with surfactant. However, the increase in I_{DS} magnitude is advantageous towards the improvement of signal-to-noise ratio in practical applications.

3.5.2 Effect of monomer: template ratio on sensor response: There have been several works showing that the response of the MIP changes if the monomer to template molar ratio in the MIP is altered [32, 33]. It is one of the possible approaches to increase the linear dynamic range of the MIP. In the previous sections, the monomer to template molar ratio is set at 6. In order to achieve a larger linear dynamic range, we synthesized two MIP with *R*=4 and *R*=8 respectively, where, $R = \frac{\text{No. of moles of monomer}}{\text{No. of moles of template}}$. The response of the sensor using these two MIP is illustrated in Fig. 10. There is no trend observed for the N.C. vs. analyte concentration curve with the *R*=4 MIP. On the other hand, we clearly observe an increasing trend in the N.C. vs. analyte concentration curve with the *R=8* MIP. There is a clear evidence of a linear dynamic range between 50 µg/L and 100 µg/L. This range is twice as large as that of the *R*=6 MIP. However, there is a downside to using this approach to increase the linear dynamic range. With *R*=8 MIP, the sensitivity is diminished as the ability to detect at 25 µg/L is lost. Nevertheless, this is a useful approach for practical sensors if the approximate concentration range of the analyte is known prior to the measurement.

3.5.3 Effect of monomer: To investigate the effect of the functional monomer constituting the MIP, a MIP using acrylic acid (poly-acrylic acid) as the monomer is synthesized. The molar ratios (*R*=6) and the synthesis procedures are identical to that of poly-acrylamide. Acrylic acid is chosen as the candidate due to its similarity with acrylamide. The only difference between the two monomers is the amide group in acrylamide is replaced by a hydroxyl group in acrylic acid. The response of the sensor with poly-acrylic acid is compared with that of poly-acrylamide in Fig. 11c. The response of poly-acrylic acid MIP is considerably small compared to that of poly-acrylamide MIP. An interesting observation is that poly-acrylic acid MIP shows a linear dynamic range between 50 µg/L and 200 µg/L. This suggests that the linear dynamic range of the MIP is adjustable via choice of the functional monomer.

3.6 Calibration curve of sensor with DEHP samples mixed with artificial saliva: To analyze phthalate migration from plastic toys, many techniques are used to simulate the sucking action by children. One such technique involves ultra-sonication of the toy samples in artificial saliva followed by quantification of phthalate concentration in the artificial saliva. However, the phthalate yield from such tests is extremely low [34]. Due to this, only laboratory based equipment such as GC-MS can be used for the quantification studies. However, we believe that our sensor could be used to detect such low levels. To verify this, the sensor is calibrated for DEHP diluted in artificial saliva. The calibration curve is shown in Fig. 12. A response is observed at 25 µg/L with a liner dynamic range between 25 µg/L and 50 µg/L, rendering this sensor suitable for application in phthalate migration tests.

4.0 Conclusion

To summarize, a molecularly imprinted polymer (MIP) functionalized extended gate field effect transistor sensor has been demonstrated for the purpose of analyzing di-2-ethylhexyl phthalate (DEHP). To the best of our knowledge, this is the first time such a device has been reported. The sensing mechanism is explained by the change in relative permittivity of the MIP upon selective capture of the analyte within the voids which results in a change in the source-drain current of the FET. The sensor exhibits a response to the analyte mixed in 2 different solvents namely n-hexanol and DI water with the sensor displaying excellent selectivity in DI water. The sensor is much more sensitive to the analyte diluted in DI water owing to the more efficient analyte capture. However, this leads to a small linear dynamic range. The linear dynamic response range has been tuned adjusting the monomer-to-template ratio (*R*) or by synthesizing the MIP with different functional monomers. Furthermore, changing the MIP loading has no effect on the

linear dynamic range. Finally, sensor exhibits response to analyte diluted in artificial saliva showing applicability in phthalate migration tests.

5.0 References

[1] B.C. DIRECTIVE, of 27 July 1976 on the approximation of the laws of the Member States relating to cosmetic products, (2003).

[2] H. Ohtani, I. Miura, Y. Ichikawa, Effects of dibutyl phthalate as an environmental endocrine disruptor on gonadal sex differentiation of genetic males of the frog Rana rugosa, Environmental Health Perspectives, 108(2000) 1189.

[3] T. Schettler, Human exposure to phthalates via consumer products, International journal of andrology, 29(2006) 134-9; discussion 81-5.

[4] R. Hauser, A. Calafat, Phthalates and human health, Occupational and environmental medicine, 62(2005) 806-18.

[5] J. Fontelles, C. Clarke, Directive 2005/84/EC of the European Parliament and of the Council of 14 December 2005 amending for the 22nd time Council Directive 76/69/EEC on the approximation of the laws, regulations and administrative provisions of the Men Der States relating to restrictions on the marketing and use of certain dangerous substances and preparations (phthalates in toys and childcare articles), Official Journal of the European Union, 48(2005) 40-3.

[6] J. Yang, R. Hauser, R.H. Goldman, Taiwan food scandal: The illegal use of phthalates as a clouding agent and their contribution to maternal exposure, Food and chemical toxicology, 58(2013) 362-8.

[7] P.-G. Wu, X.-D. Pan, B.-J. Ma, L.-Y. Wang, J. Zhang, Determination of phthalate esters in non-alcoholic beverages by GC–MS and optimization of the extraction conditions, European Food Research and Technology, 238(2014) 607-12.

[8] A. Mousa, C. Basheer, A. Rahman Al-Arfaj, Determination of phthalate esters in bottled water using dispersive liquid–liquid microextraction coupled with GC–MS, Journal of separation science, 36(2013) 2003-9.

[9] J. Du, R. Gao, H. Mu, A Novel Molecularly Imprinted Polymer Based on Carbon Nanotubes for Selective Determination of Dioctyl Phthalate from Beverage Samples Coupled with GC/MS, Food Analytical Methods, (2015) 1-10.

[10] Y. Jiao, S. Fu, L. Ding, Q. Gong, S. Zhu, L. Wang, et al., Determination of trace leaching phthalate esters in water by magnetic solid phase extraction based on magnetic multi-walled carbon nanotubes followed by GC-MS/MS, Analytical Methods, 4(2012) 2729-34.

[11] M. Wagner, J. Oehlmann, Endocrine disruptors in bottled mineral water: total estrogenic burden and migration from plastic bottles, Environmental Science and Pollution Research, 16(2009) 278-86.

[12] X.-L. Cao, Determination of phthalates and adipate in bottled water by headspace solid-phase microextraction and gas chromatography/mass spectrometry, Journal of Chromatography A, 1178(2008) 231-8.

[13] G. Leng, W. Chen, M. Zhang, F. Huang, Q. Cao, Determination of phthalate esters in liquor samples by vortex-assisted surfactant-enhanced-emulsification liquid–liquid microextraction followed by GC–MS, Journal of separation science, 37(2014) 684-90.

[14] G. Prokůpková, K. Holadová, J. Poustka, J. Hajšlová, Development of a solid-phase microextraction method for the determination of phthalic acid esters in water, Analytica Chimica Acta, 457(2002) 211-23.

[15] C.-W. Ye, J. Gao, C. Yang, X.-J. Liu, X.-J. Li, S.-Y. Pan, Development and application of an SPME/GC method for the determination of trace phthalates in beer using a calix [6] arene fiber, Analytica chimica acta, 641(2009) 64-74.

[16] W. Ling, G.-b. JIANG, Y.-q. CAI, H. Bin, Y.-w. WANG, D.-z. SHEN, Cloud point extraction coupled with HPLC-UV for the determination of phthalate esters in environmental water samples, Journal of Environmental Sciences, 19(2007) 874-8.

[17] X. Ye, Z. Kuklenyik, L.L. Needham, A.M. Calafat, Automated on-line column-switching HPLC-MS/MS method with peak focusing for the determination of nine environmental phenols in urine, Analytical chemistry, 77(2005) 5407-13.

[18] B.C. Blount, K.E. Milgram, M.J. Silva, N.A. Malek, J.A. Reidy, L.L. Needham, et al., Quantitative detection of eight phthalate metabolites in human urine using HPLC-APCI-MS/MS, Analytical Chemistry, 72(2000) 4127-34.

[19] Y. Hayasaka, Analysis of phthalates in wine using liquid chromatography tandem mass spectrometry combined with a hold-back column: Chromatographic strategy to avoid the influence of pre-existing phthalate contamination in a liquid chromatography system, Journal of Chromatography A, 1372(2014) 120-7.

[20] A.I. Zia, A.M. Syaifudin, S. Mukhopadhyay, I. Al-Bahadly, P. Yu, C.P. Gooneratne, et al., MEMS based impedimetric sensing of phthalates, 2013 IEEE International Instrumentation and Measurement Technology Conference (I2MTC), IEEE2013, pp. 855-60.

[21] A.I. Zia, A.M. Syaifudin, S. Mukhopadhyay, I. Al-Bahadly, P. Yu, C. Gooneratne, et al., Development of Electrochemical Impedance Spectroscopy based sensing system for DEHP detection, Sensing Technology (ICST), 2011 Fifth International Conference on, IEEE2011, pp. 666-74.

[22] A.I. Zia, M.S.A. Rahman, S.C. Mukhopadhyay, P.-L. Yu, I.H. Al-Bahadly, C.P. Gooneratne, et al., Technique for rapid detection of phthalates in water and beverages, Journal of Food Engineering, 116(2013) 515-23.

[23] A.I. Zia, S.C. Mukhopadhyay, P.-L. Yu, I.H. Al-Bahadly, C.P. Gooneratne, J. Kosel, Rapid and molecular selective electrochemical sensing of phthalates in aqueous solution, Biosensors and Bioelectronics, 67(2015) 342-9.

[24] P. Bergveld, Thirty years of ISFETOLOGY: What happened in the past 30 years and what may happen in the next 30 years, Sensors and Actuators B: Chemical, 88(2003) 1-20.

[25] S. Ji, Q.-J. Sun, S. Venkatesh, Y. Yan, Y. Zhou, J. Zhuang, et al., Low-voltage extended gate organic thin film transistors for ion sensing based on semi-conducting polymer electrodes, SPIE OPTO, International Society for Optics and Photonics2016, pp. 974912--8.

[26] C. Celle, C. Suspène, M. Ternisien, S. Lenfant, D. Guérin, K. Smaali, et al., Interface dipole: Effects on threshold voltage and mobility for both amorphous and poly-crystalline organic field effect transistors, Organic Electronics, 15(2014) 729-37.

[27] Y. Yoshimi, R. Ohdaira, C. Iiyama, K. Sakai, “Gate effect” of thin layer of molecularly-imprinted poly (methacrylic acid-co-ethyleneglycol dimethacrylate), Sensors and Actuators B: Chemical, 73(2001) 49-53.

[28] R. Ouyang, J. Lei, H. Ju, Y. Xue, A molecularly imprinted copolymer designed for enantioselective recognition of glutamic acid, Advanced Functional Materials, 17(2007) 3223-30.

[29] G. Ertürk, M. Hedström, B. Mattiasson, A sensitive and real-time assay of trypsin by using molecular imprinting-based capacitive biosensor, Biosensors and Bioelectronics, 86(2016) 557-65.

[30] T. Yao, X. Gu, T. Li, J. Li, J. Li, Z. Zhao, et al., Enhancement of surface plasmon resonance signals using a MIP/GNPs/rGO nano-hybrid film for the rapid detection of ractopamine, Biosensors and Bioelectronics, 75(2016) 96-100.

[31] R. Pernites, R. Ponnapati, M.J. Felipe, R. Advincula, Electropolymerization molecularly imprinted polymer (E-MIP) SPR sensing of drug molecules: Pre-polymerization complexed terthiophene and carbazole electroactive monomers, Biosensors and Bioelectronics, 26(2011) 2766-71.

[32] E. Yilmaz, K. Mosbach, K. Haupt, Influence of functional and cross-linking monomers and the amount of template on the performance of molecularly imprinted polymers in binding assays, Analytical Communications, 36(1999) 167-70.

[33] K. Yoshimatsu, T. Yamazaki, I.S. Chronakis, L. Ye, Influence of template/functional monomer/cross-linking monomer ratio on particle size and binding properties of molecularly imprinted nanoparticles, Journal of Applied Polymer Science, 124(2012) 1249-55.

[34] F. Fiala, I. Steiner, K. Kubesch, Migration of di-(2-ethylhexyl) phthalate (DEHP) and diisononyl phthalate (DINP) from PVC articles, Deutsche Lebensmittel Rundschau, 96(2000) 51-7.

Acknowledgements

We would like to acknowledge Mr. Daniel Yau for technical support. We acknowledge the grants from City University of Hong Kong project number 7004378.

Competing financial interests

The authors declare no competing financial interest.

Figures

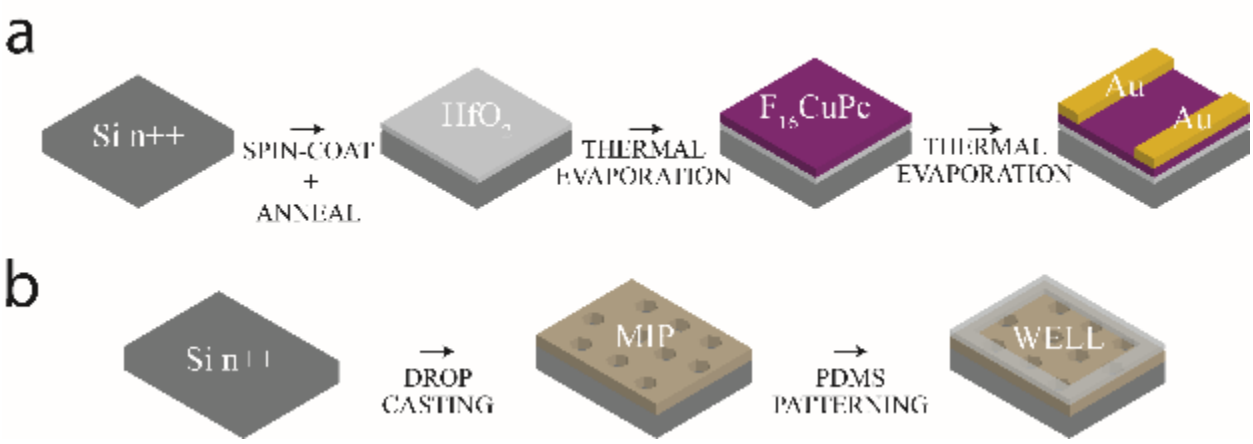

Fig 1. (a) Illustration of the fabrication procedure for the OFET. (b) Illustration figure for the fabrication of the extended gate sensor.

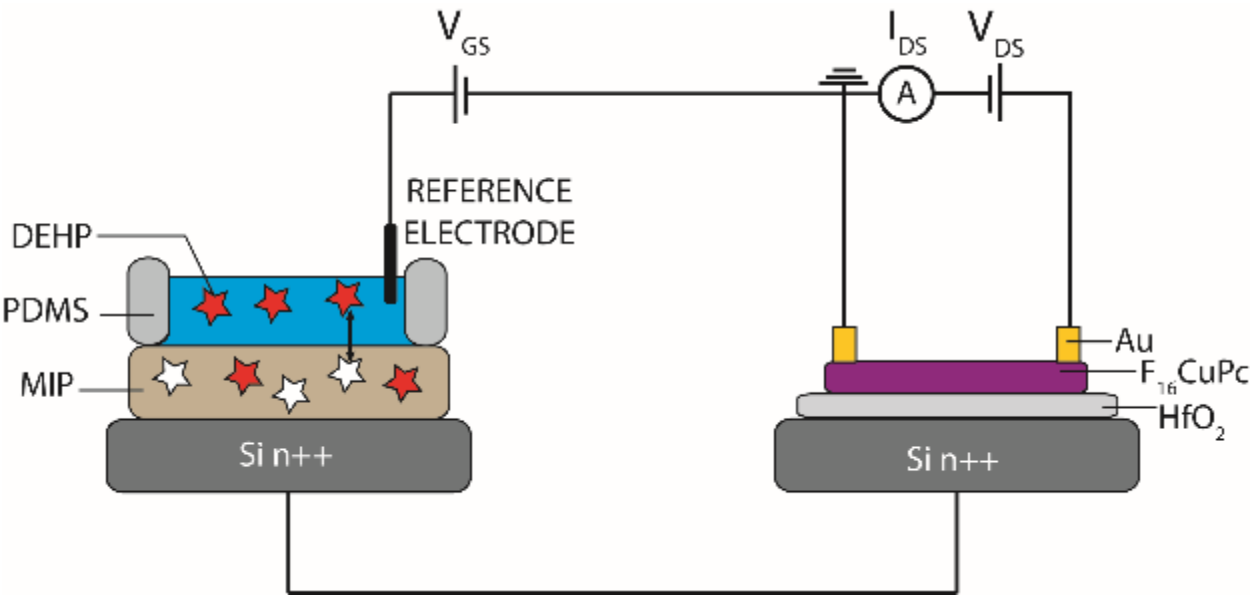

Fig. 2. Illustration of the extended gate sensor structure. The bottom gate of the OFET is connected to the heavily doped silicon substrate of the extended gate sensor. The gate voltage (V_{GS}) is supplied through the reference electrode immersed in the sample. The drain voltage (V_{DS}) is applied to the OFET and the source-drain current (I_{DS}) is measured from the OFET.

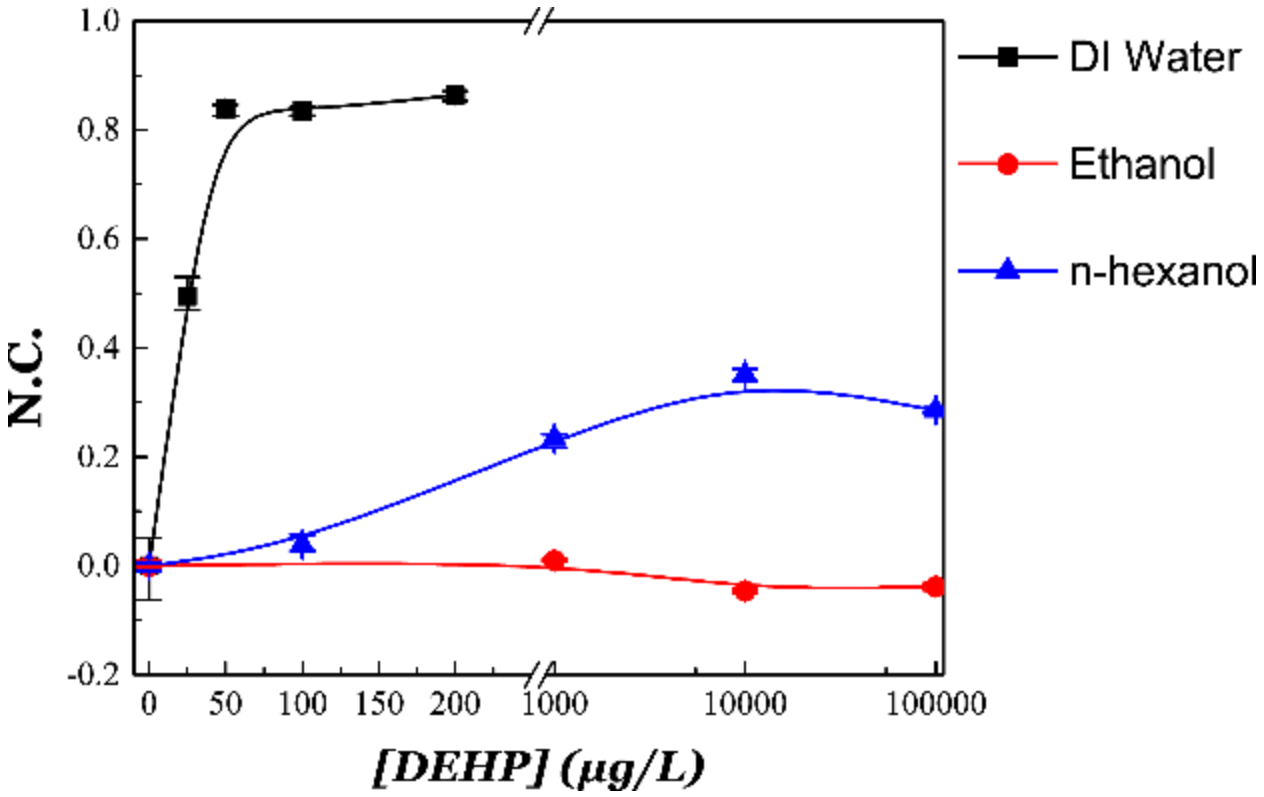

Fig. 3. Response of the sensor as a function of N.C. to various concentration of DEHP in DI water, n-hexanol and ethanol. The gate voltage and the drain voltage are kept at a value of 3V during the test.

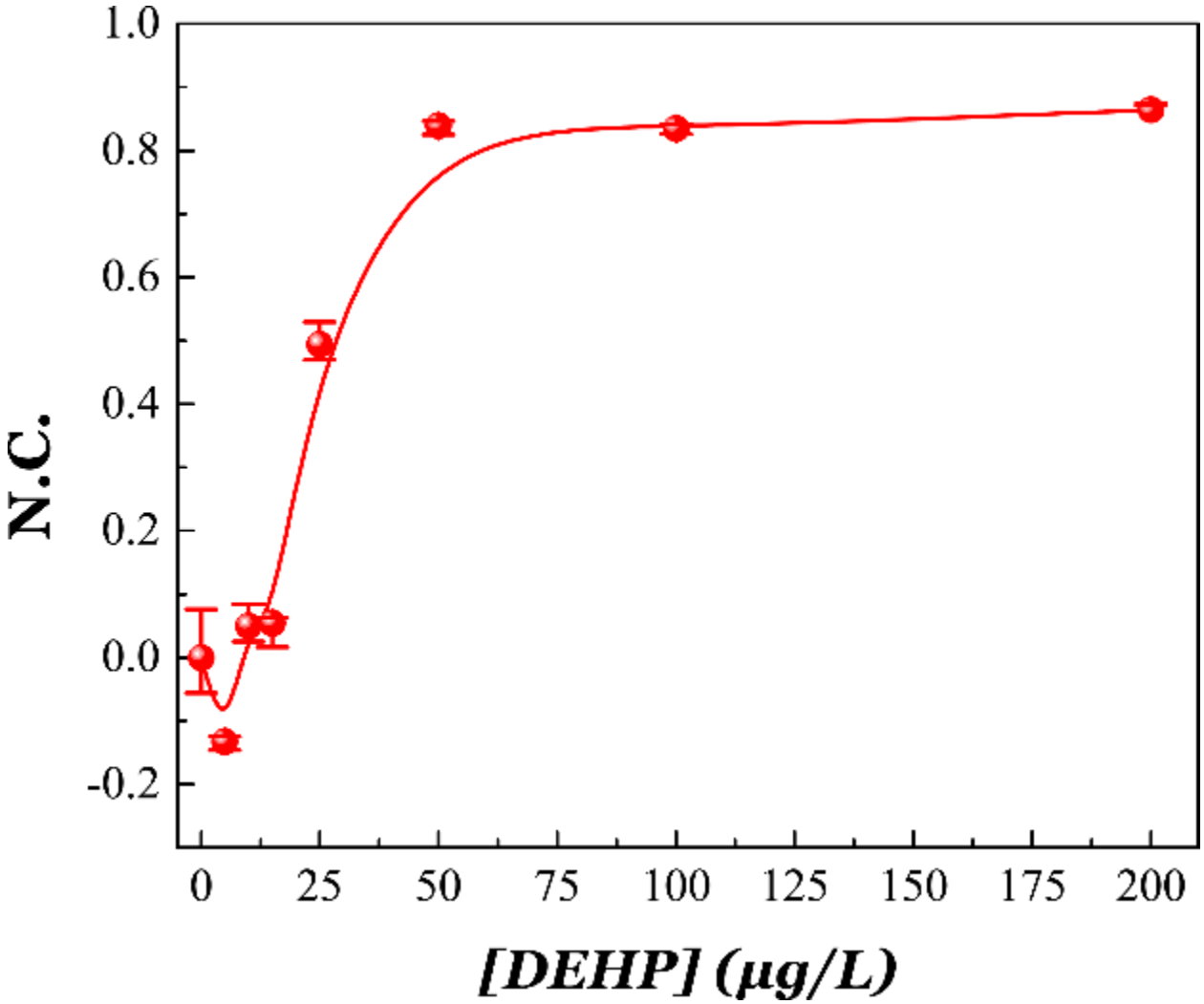

Fig. 4. Calibration of the sensor with DEHP samples dissolved in water. The error bars show the maximum and minimum values from the experiment.

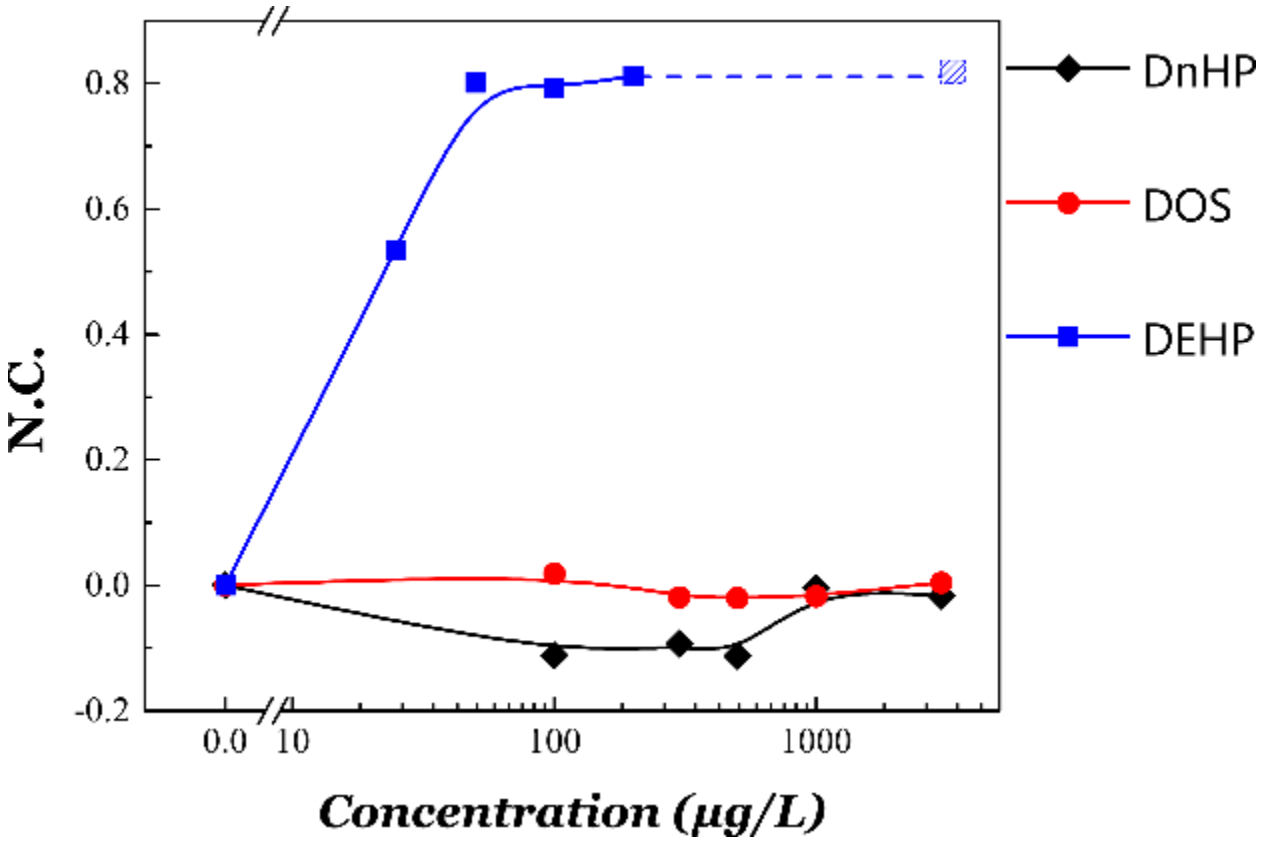

Fig. 5. Calibration of the sensor with DEHP, dioctyl sebacate (DOS) and DnHP (di-n-hexyl phthalate) samples dissolved in water. The sensor shows a distinguishable response for DEHP indicating specific analyte capture by the MIP. The dashed blue line and the blue box represents the predicted response of the sensor to DEHP at 2000 µg/L (shown as a flat line due to the saturation of the MIP at 50 µg/L).

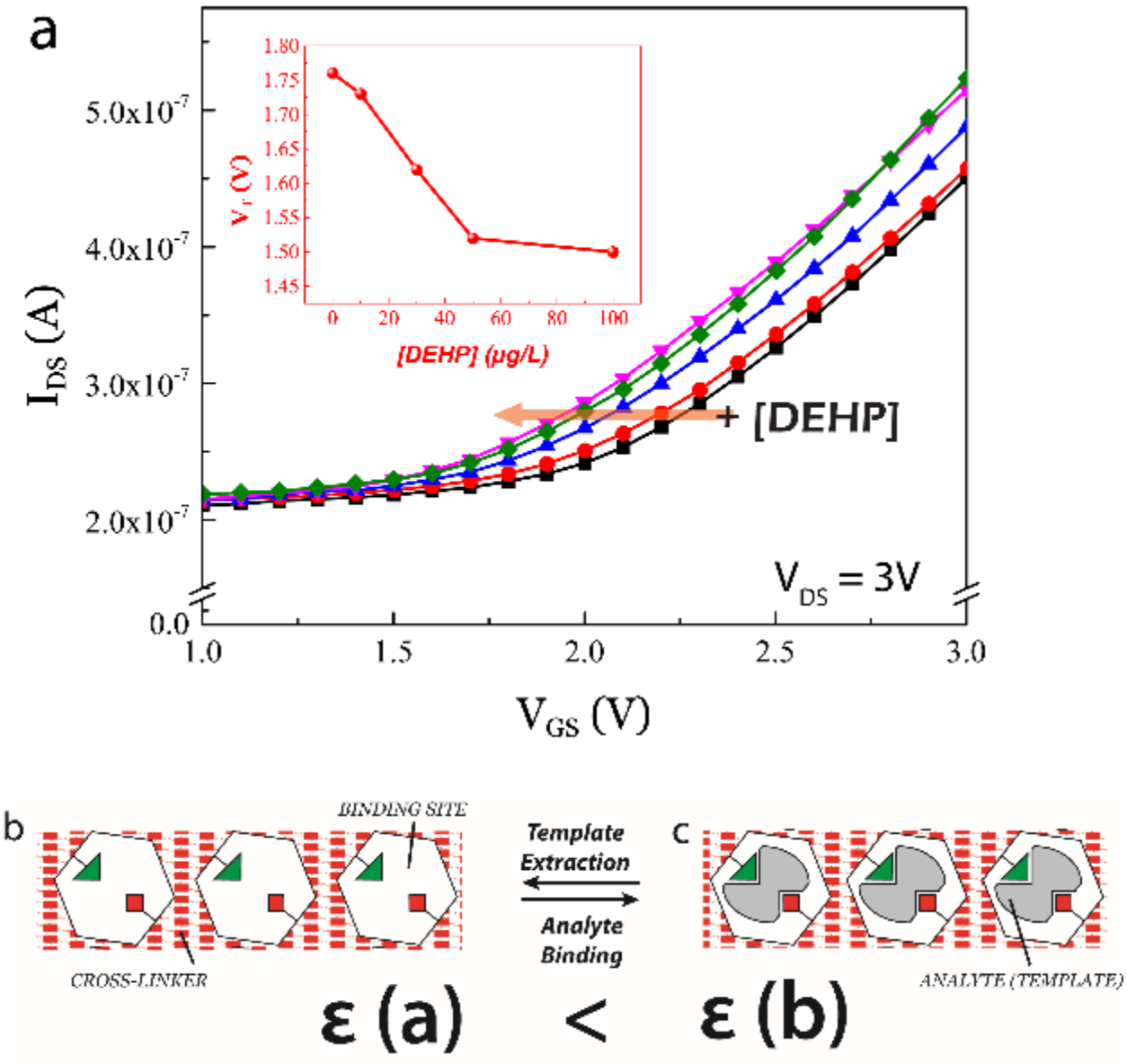

Fig. 6. (a) I_{DS}-V_{GS} (Transfer) curves of the extended gate sensor when exposed to different concentrations of 0-100 µg/L DEHP analyte. The drain voltage (V_{DS}) is kept constant at 3V while the gate voltage swept at a rate of 0.1V/s. The threshold voltage decreases with increasing DEHP concentration. The inset shows the dependence of the threshold voltage (V_T) on the concentration of DEHP. Schematic showing the **(b)** template extraction (during the MIP synthesis) and **(c)** analyte binding during the tests. The occupation of the binding site by the analyte increases the relative permittivity (ε) of the MIP leading to the increase in capacitance of

the MIP. This increase in capacitance is induced into an electrical signal (source-drain current) by the extended gate sensor.

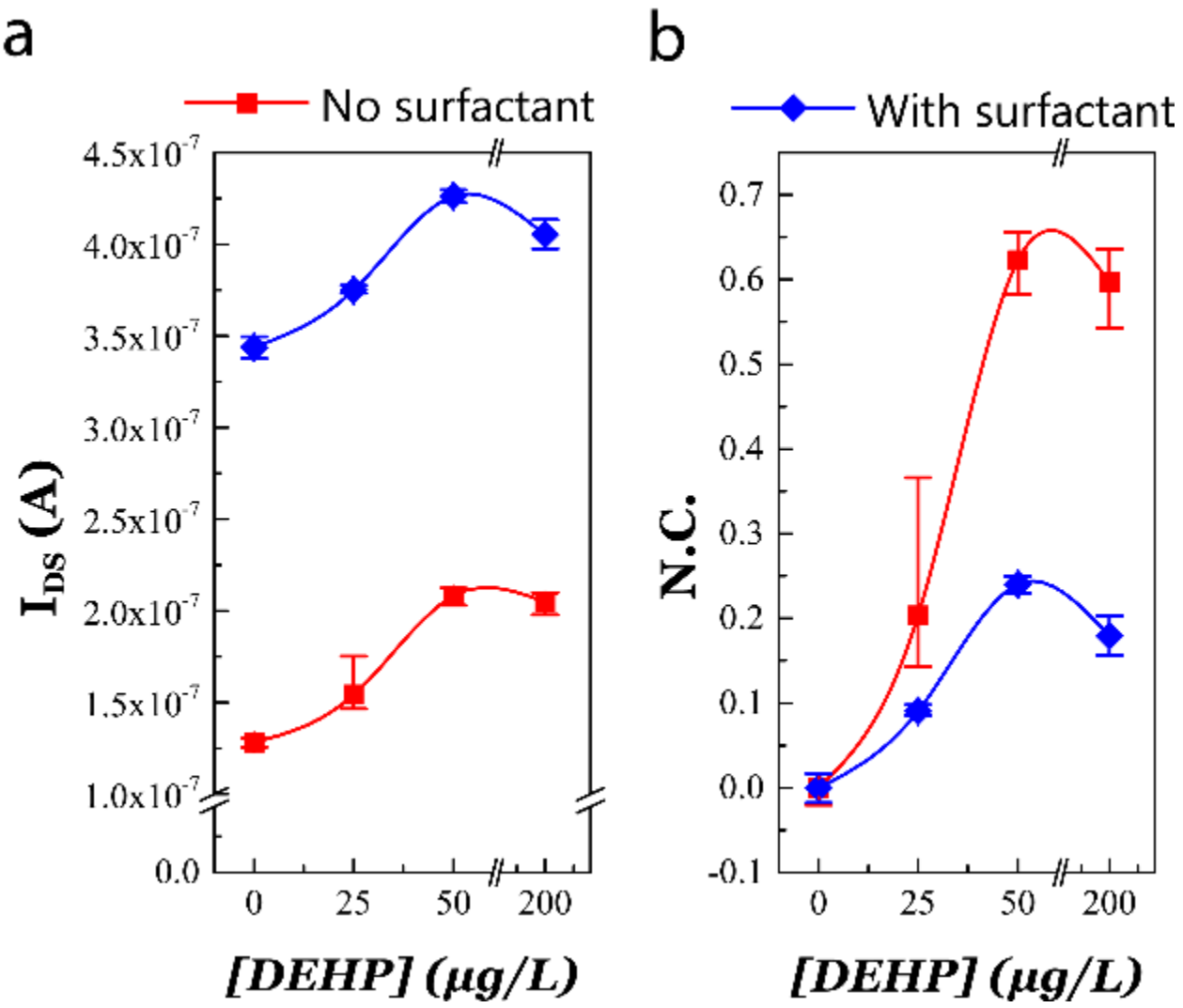

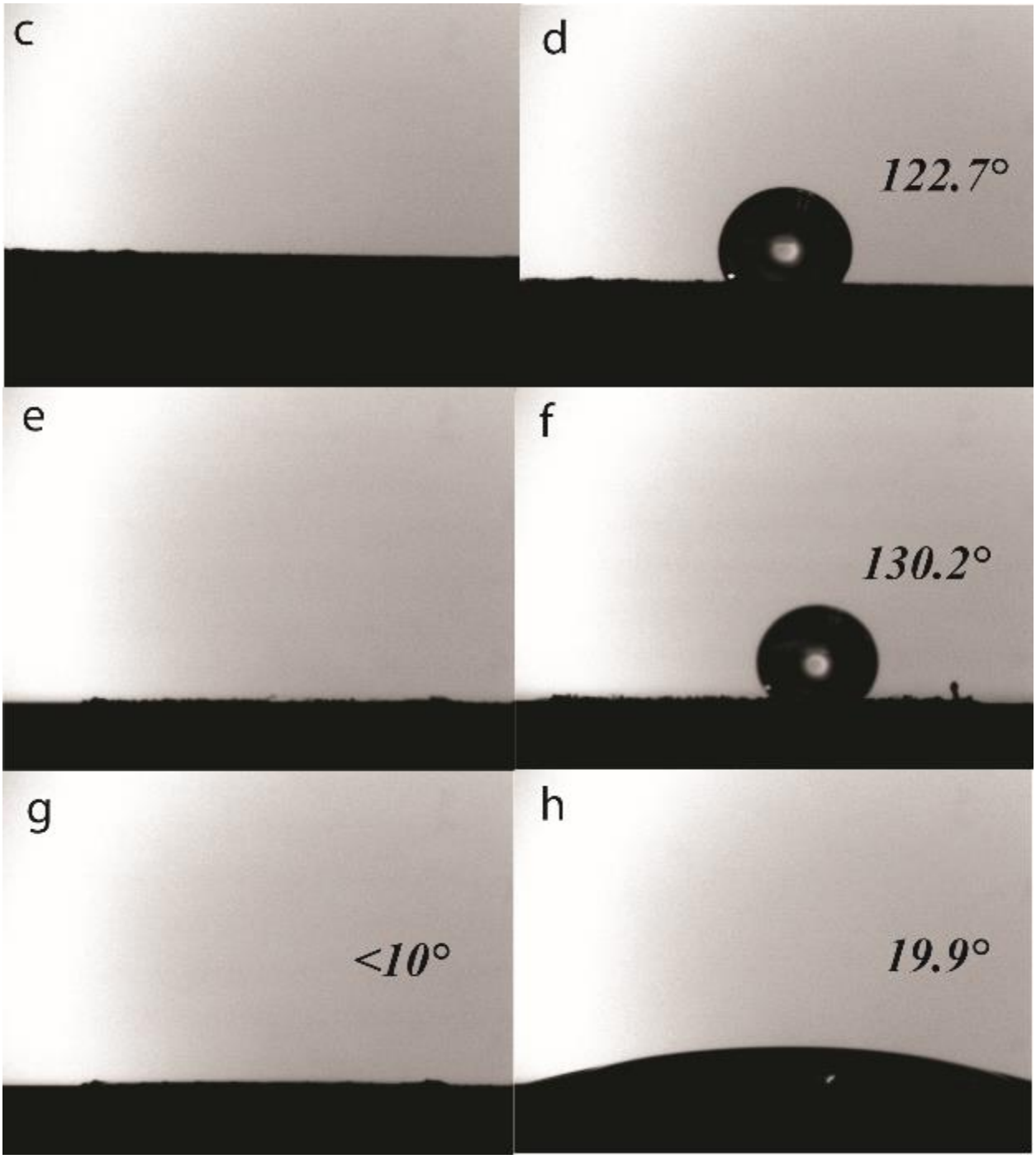

Fig. 7. Calibration curves as a function of **(a)** I_{DS} and **(b)** N.C. for sensor with MIP loading at 5 mg/mL. The I_{DS} is recorded while keeping $V_{DS}=V_{GS}=$ 3V. Contact angle goniometer images. **(c)** Bare surface of MIP with a loading of 1mg/mL **(d)** 2 µL of DI water on 1mg/mL MIP loaded surface. **(e)** Bare surface of MIP with a loading of 5 mg/mL. **(f)** 2 µL of DI water on 5 mg/mL

MIP loaded surface. **(g)** 2 µL of DI water mixed with 0.5% surfactant on 5 mg/mL MIP loaded surface. **(h)** 6 µL of DI water mixed with 0.5% surfactant on 5 mg/mL MIP loaded surface.

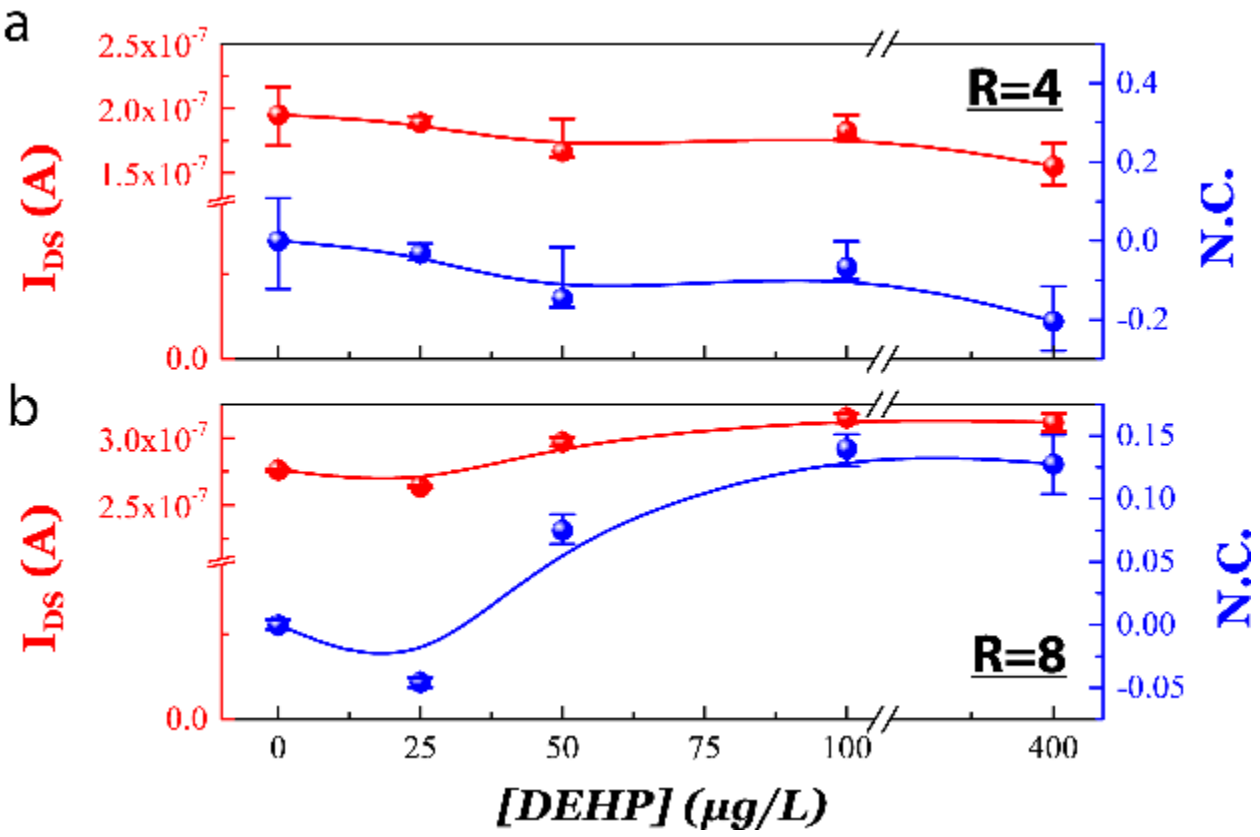

Fig. 8. Calibration curves as a function of I_{DS} and N.C. for sensor with MIP monomer to template molar ratio, R, at **(a)** R= 4 & **(b)** R=8. The I_{DS} is recorded while keeping V_{DS}=V_{GS}= 3V.

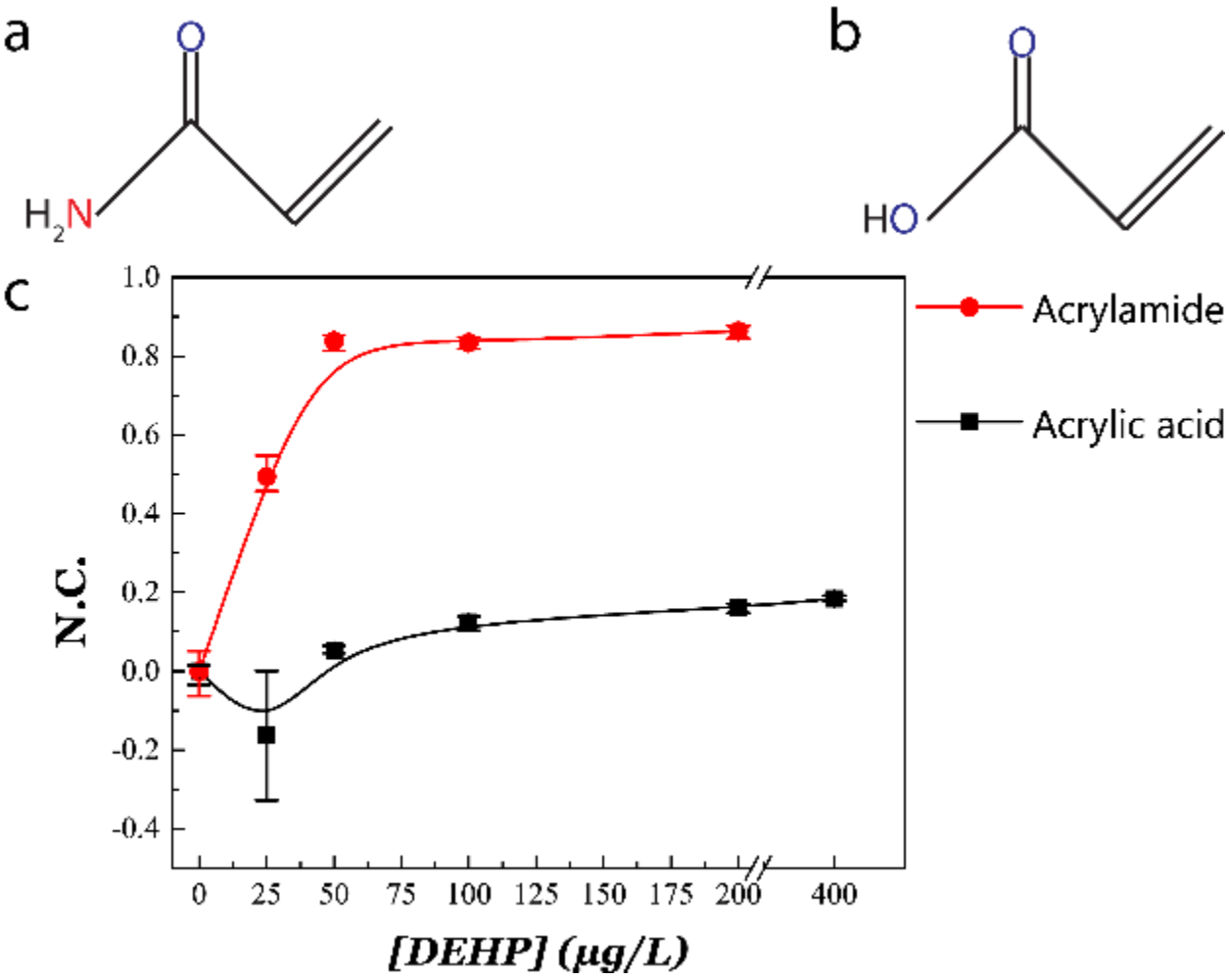

Fig. 9. Schematic showing the structure of the functional monomers **(a)** acrylamide and **(b)** acrylic acid. **(c)** The calibration curve of DEHP dissolved in water as a function of N.C utilizing MIPs synthesized with the three different functional monomers. The MIP loading in all three cases is 1mg/mL. The monomer-to-template ratio is all three cases is *R*=6. The I_{DS} is recorded while keeping V_{DS}=V_{GS}= 3V.

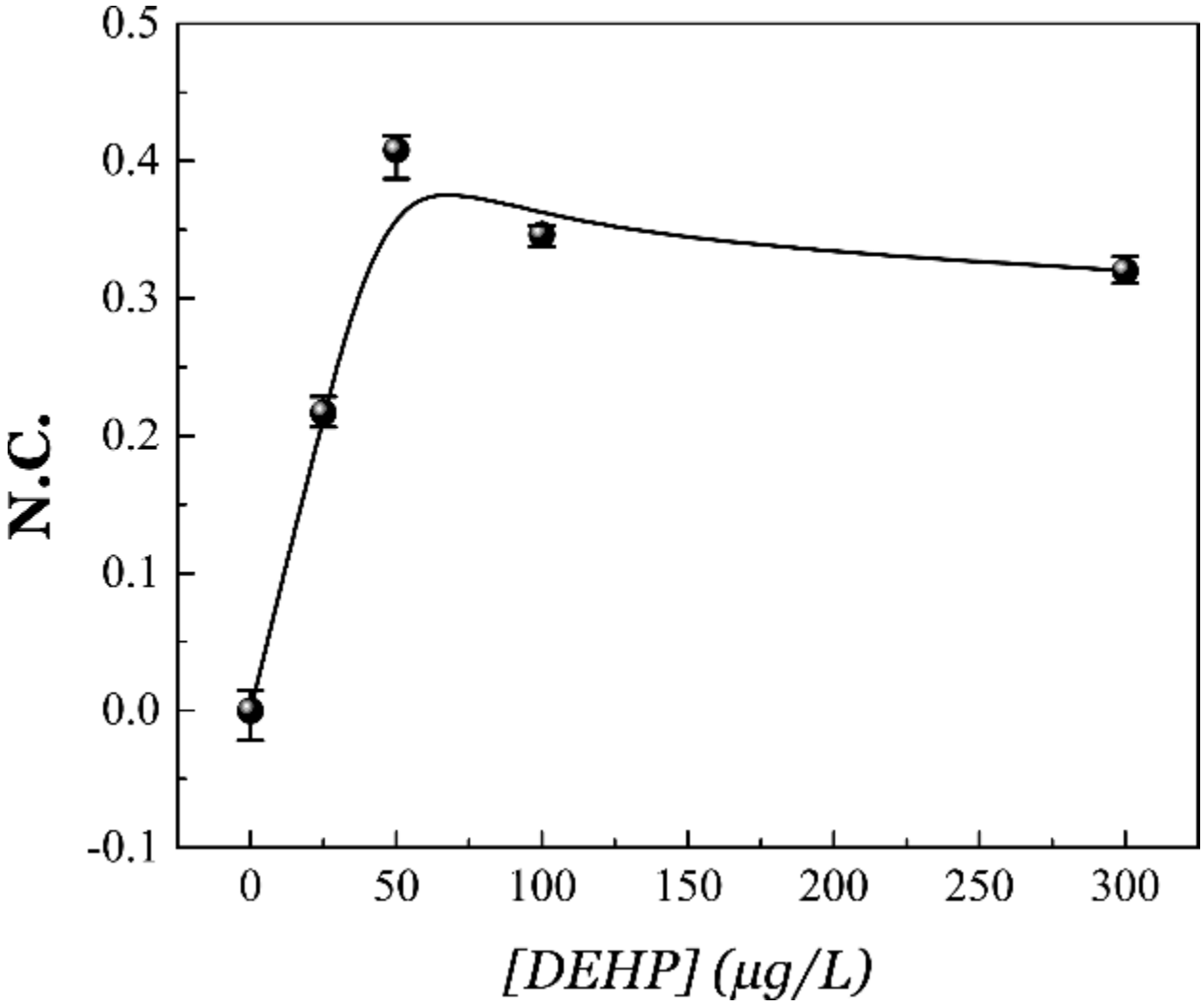

Fig. 10. Calibration of the sensor with DEHP samples dissolved in artificial saliva. The black spheres with the error bars represent the actual data points from the experiment. The black line is best fit spline for the data points. Each concentration was tested twice. The center of the sphere is represents the average value while the error bars show the maximum and minimum values from the experiment.